Observation of Anomalous Orbital Angular Momentum Transfer in Parametric Nonlinearity

Hai-Jun Wu,[1] Bing-Shi Yu,[1] Jia-Qi Jiang,[1] Chun-Yu Li,[1] Carmelo Rosales-Guzmán,[1,2] Shi-Long Liu,[3] Zhi-Han Zhu,[1,*] and Bao-Sen Shi[1,4,†]

[1]*Wang Da-Heng Center, HLG Key Laboratory of Quantum Control, Harbin University of Science and Technology, Harbin 150080, China*
[2]*Centro de Investigaciones en Óptica, A.C., Loma del Bosque 115, Colonia Lomas del Campestre, 37150 León, Gunajuato, Mexico*
[3]*FemtoQ Lab, Engineering Physics Department, Polytechnique Montréal, Montréal, Québec H3T 1JK, Canada*
[4]*CAS Key Laboratory of Quantum Information, University of Science and Technology of China, Hefei 230026, China*

(Received 23 October 2022; accepted 27 March 2023; published 14 April 2023)

Orbital angular momentum (OAM) conservation plays an important role in shaping and controlling structured light with nonlinear optics. The OAM of a beam originating from three-wave mixing should be the sum or difference of the other two inputs because no light–matter OAM exchange occurs in parametric nonlinear interactions. Here, we report anomalous OAM transfer in parametric upconversion, in which a Hermite-Gauss mode signal interacts with a specially engineered pump capable of astigmatic transformation, resulting in Laguerre-Gaussian mode sum-frequency generation (SFG). The anomaly here refers to the fact that the pump and signal both carry no net OAM, while their SFG does. We reveal experimentally that there is also an OAM inflow to the residual pump, having the same amount of that to the SFG but with the opposite sign, and thus holds system OAM conservation. This unexpected OAM selection rule improves our understanding of OAM transfer among interacting waves and may inspire new ideas for controlling OAM states via nonlinear optics.

DOI: 10.1103/PhysRevLett.130.153803

Since Franken *et al.* first discussed nonlinear optics more than sixty years ago, optical parametric nonlinearity has been extensively studied due to its irreplaceable potential in controlling the temporal frequency (or longitudinal mode) of light [1]. The term "parametric" refers to the excited nonlinear polarization being an instantaneous virtual level, with the light-matter interaction not changing the quantum state of the medium [2]. This indicates that energy and momentum are conserved in light fields and, crucially, that the conservation law governs frequency conversion and the associated phase-matching conditions. With the increased understanding of orbital angular momentum (OAM) and structured light over the last three decades [3–5], shaping the spatial structure of light with nonlinear optics has gradually become a fascinating subject in the research community [6–8]. In addition to phase matching and polarization dependence, the effect of momentum conservation on nonlinear interactions also includes crucial contributions from OAM conservation, which has a nontrivial impact on the spatial structures of interacting beams. Thus, soon after Allen *et al.* discovered optical OAM [3], several scientists investigated the second-harmonic generation of Laguerre-Gaussian (LG) modes, noting that harmonic beams carry twice the topological charge (representing the OAM per photon) of the input. This pioneering observation provided straightforward insight into OAM conservation in parametric interactions and, more importantly, led to the development of a nonlinear optic paradigm of how OAM transfers between light [9]. Namely, the OAM of a new beam originating from a parametric interaction is always determined by the topological-charge arithmetic of the input beams.

For instance, the OAM of a newly generated wave in a three-wave mixing is determined by the sum or difference of the OAM (with respect to the new generated beam's axis) of the other two inputs. Thereafter, the transfer of OAM among interacting waves (or the OAM selection rule) was widely studied in nearly all known parametric processes including both collinear and noncollinear schemes, from photon-level quantum interactions to ultrafast and intense-field regions, and OAM transfer between light and matter waves has also been considered [10–20]. The scope of relevant studies has recently been extended from solo OAM degree of freedom to encompass spin-orbit coupling and spatiotemporal vortices [21–28]. Beyond fundamental studies, the nonlinear transfer of vortex phase exhibited also potential in light-field shaping and imaging processing [29–32].

Remarkably, however, previous results all follow the rooted paradigm proposed by the pioneering work. In this work, we report an unexpected *anomalous* OAM conservation in a second-order parametric nonlinear system, in which

Hermite-Gaussian (HG) signals are upconverted to the corresponding LG modes by a specially engineered pump beam capable of astigmatic transformation. Compared with the current paradigm, the *anomaly* here occurs in the origin of the OAM inflows in the new generated beam, i.e., the two inputs have both no net OAM, but their sum-frequency generation does out of the blue. This unexpected result extends our current understanding of OAM conservation and may provide new insight into the nonlinear control of OAM states.

To understand the principle of nonlinear astigmatic transformation (AT), we first revisit how to convert a correlated pair of Hermite-Laguerre-Gauss (HLG) modes, denoted as $\mathrm{LG}_{\ell,p}$ and $\mathrm{HG}_{m,n}$, on the same modal sphere with the order $N = 2p + |\ell| = m + n$. The crucial mathematical relation that allows the conversion is that $\mathrm{LG}_{\ell,p}$ and a diagonally placed $\mathrm{HG}^{45°}_{m,n}$ can both be represented using the superposition states of all N-order HG modes [33–36]. For simplicity, taking the two-order HLG modes as an example

$$\mathrm{HG}^{45°}_{1,0} = \sqrt{1/2}(\mathrm{HG}_{1,0} + \mathrm{HG}_{0,1}), \tag{1}$$

$$\mathrm{LG}_{1,0} = \sqrt{1/2}(\mathrm{HG}_{1,0} + i\mathrm{HG}_{0,1}). \tag{2}$$

The conversion from Eqs. (1) to (2) requires introducing a $\pm\pi/2$ intramodal phase between the two components. This unitary transformation can be achieved by exploiting the axial separability of the Gouy phase in Cartesian coordinates [34]

$$(N+1)\phi = (m+1/2)\phi_x + (n+1/2)\phi_y, \tag{3}$$

where ϕ and $\phi_{x,y}$ denote the Gouy phase and its axial components, respectively [37]. This approach mimics the rotational quarter-wave plate used in polarization control [35,36]. The true zero-order AT operations can be realized by using fractional Fourier transformations based on phase-only modulation [41,42]. Figure 1(a) shows the principle of the AT convertor, which includes two cascading phase masks $v(\boldsymbol{r})$, as well as the beam evolution of an example mode during the conversion [37]. When a diagonal $\mathrm{HG}_{1,0}$ mode passes through the convertor, the Gouy phases accumulated in the x and y planes are $\pi/4$ and $3\pi/4$, respectively. Thus, we have $\phi_y - \phi_x = \pi/2$, and, consequently, the output beam can be converted into $\mathrm{LG}_{1,0}$, and vice versa.

In addition to modal conversion, a crucial concern in connection with OAM conservation is how the OAM transfers between the light and phase masks. In polarization control, the phase retardation and associated spin transfer gradually accumulates during birefringence propagation. However, the AT operation is entirely different, as the OAM transfer is completed in AT_1 at the HG port [34]. This conclusion can be examined by the change in the OAM spectrum, i.e., by decomposing the astigmatic beam as a set of LG modes $\sum c_{\ell,p}\mathrm{LG}_{\ell,p}$. For instance, Eq. (1) becomes $\mathrm{HG}^{45°}_{1,0}(\boldsymbol{r})e^{iv(\boldsymbol{r})}$ as the beam passes through AT_1, as shown in Fig. 1(b), leading to the spectrum broader than its original. More importantly, the spectrum becomes asymmetric with respect to $\ell = 0$, indicating the astigmatic beam carries already net OAM, with an average OAM of $-1\hbar$ per photon. As the beam propagates near AT_2, the intramodal phases between successive LG components have been modulated by the Gouy phase [43,44]. As a result, the beam structure is reshaped into an astigmatic $\mathrm{LG}_{\ell,0}$ mode. Then, AT_2 recovers it as a standard $\mathrm{LG}_{\ell,0}$ mode by removing the astigmatic wave front, which is equivalent to compressing the OAM spectrum into a single value $\ell = -1$.

On the basis of the above explanation, Fig. 1(c) shows a schematic of a nonlinear AT modal conversion based on sum-frequency generation (SFG). Compared with the linear

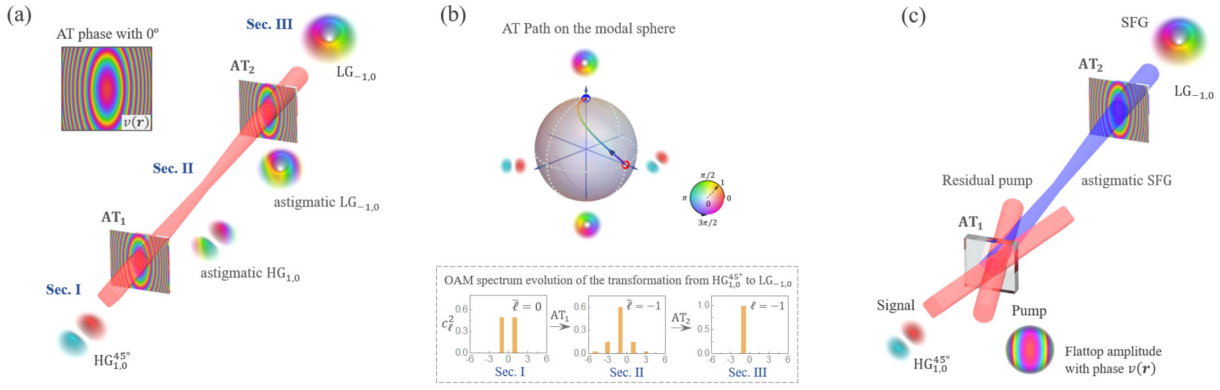

FIG. 1. Principle of the true zero-order astigmatic transformation during HG-to-LG conversion, with (a) and (c) showing schemes for linear and nonlinear optical systems, respectively, and (b) showing the AT path on the modal sphere and the associated OAM spectrum evolution.

system, the first phase mask is replaced by an upconversion system consisting of SFG crystal and AT pump. To realize a phase-only AT modulation on signal [45,46], the pump is a specially engineered beam that has a super Gaussian (or flattop) amplitude that carries the AT wave front $v(\boldsymbol{r})$, so that it can perform both frequency and AT conversions on the signal. In this astigmatic up-conversion, remarkably, the OAM conservation law appears to encounter a problem. Specifically, the pump and signal both carry no net OAM (denoted as $\ell_p = \ell_s = 0$) but their SFG originating from the crystal does ($\ell_{\mathrm{up}} \neq 0$). This finding is especially curious for the parametric system because the nonlinear polarization is virtual and there should be no OAM light-matter exchange.

In the following section, we conduct several experiments to reveal the *anomalous* OAM selection rule underlying this nonlinear AT. Note that the noncollinear scheme shown in Fig. 1(c) limits the interaction length and would lead to noninteger OAM generation [12]. Therefore, to demonstrate the selection rule unambiguously, we performed the experiment with collinear SFG in a quasiphase matching crystal, involving both small-signal and pump-depletion cases.

Figure 2 shows a schematic setup of the experiment, where we used a degenerated SFG with type-0 phase matching to build the nonlinear optics platform. A pulsed 1560 nm laser and its frequency doubling were used as the initial source to prepare the signal and pump. The signal beam was shaped into the desired HG mode, and the pump beam was designed with a special spatial structure—a flattop amplitude carrying the AT wave front $v(\boldsymbol{r})$ [37]. The prepared signal was first combined with the pump at a dichroic mirror (DM-1) and then relayed to a 15 mm-long quasi-phase matching crystal (PPKTP) via an imaging lens. The SFG from the crystal inherits the complex amplitude of the signal and the wave front $v(\boldsymbol{r})$ from the pump.

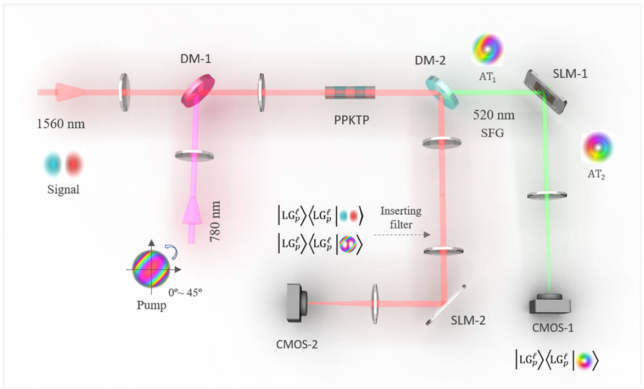

FIG. 2. Schematic representation of the experimental setup, where the key components are the dichroic mirror (DM), spatial light modulator (SLM), camera (CMOS), and periodically poled $KTiOPO_4$ (PPKTP) crystal.

At the output of the crystal, a short-pass dichroic mirror (DM-2) separates the SFG at 520 nm from the mixing waves. This signal is then characterized by a spatial spectrum analyzer composed of a 10-bit spatial light modulator (SLM-1) and a CMOS camera [47,48]. In particular, by switching the hologram type loaded on SLM-1, i.e., a solo LG projection mask or a combination mask including $v(\boldsymbol{r})$, we can measure the OAM spectrum before and after the SFG passes through AT_2. In the reflecting port of DM-2, the residual pump or seed (inserting a 780/1560 nm band pass filter) is relayed to another spatial spectrum analyzer to measure the OAM. In addition, we use a complex amplitude profiler based on spatial Stokes tomography for *in situ* observations of the full structure of the three beams. More details are provided in Ref. [37].

In the experiment, for convenience, we used a rotational AT pump to interact with horizontal HG signals instead of the rotated signal scheme shown in Fig. 1. Two low-order modes, $HG_{1,0}$ and $HG_{2,0}$, were chosen as the example signals. The angle of the AT pump with respect to the horizontal plane was set to 22.5° and 45°, to convert $HG_{1,0}$ and $HG_{2,0}$ to intermediate HLG modes and $LG_{1,0}$ and $LG_{2,0}$ modes on the modal sphere, respectively. We first consider a small signal scenario in which the amplitude of the AT pump is assumed to be constant. Figure 3 shows the measured complex amplitude and OAM spectra of the input HG signal and associated HLG and LG SFG, as well as their theoretical references [49]. To confirm the well pump-signal overlap in the crystal, the signal was measured after passing the crystal, i.e., using SLM-2, because the well-overlapped flattop pump does not change signal beam structure [45,46]. The results, including both measured OAM spectra and observed complex amplitudes, of the original HG signals, intermediate HLG and final LG SFG agree well with and thus confirmed the theory. Moreover, the amount of net OAM carried by the two SFG beams, denoted as $\ell_{\mathrm{up}}\hbar$, gradually increased to $-\hbar$ and $-2\hbar$ per photon as the angle of the AT pump increased from 22.5° to 45°. Importantly, the net OAM inflows to the SFG occurred during the first nonlinear AT operation in the crystal. The result however poses a big puzzle to the OAM conservation law in parametric nonlinear systems; namely, since the two inputs in the three-wave interaction carry no net OAM, what is the origin of the OAM inflows in the third wave during the interaction?

The SFG, as an all-optical nonlinearity, has no light-matter OAM exchange. Therefore, the only possible hideout of the undiscovered OAM that can conserve the OAM conservation in the system is the residual pump beam. The interactions with the HG modes reshape the amplitude structure of the residual pump, which may lead to this beam carrying net OAM. For experimental observation, however, the changes in the amplitude structure and associated OAM per photon are too subtle in the small

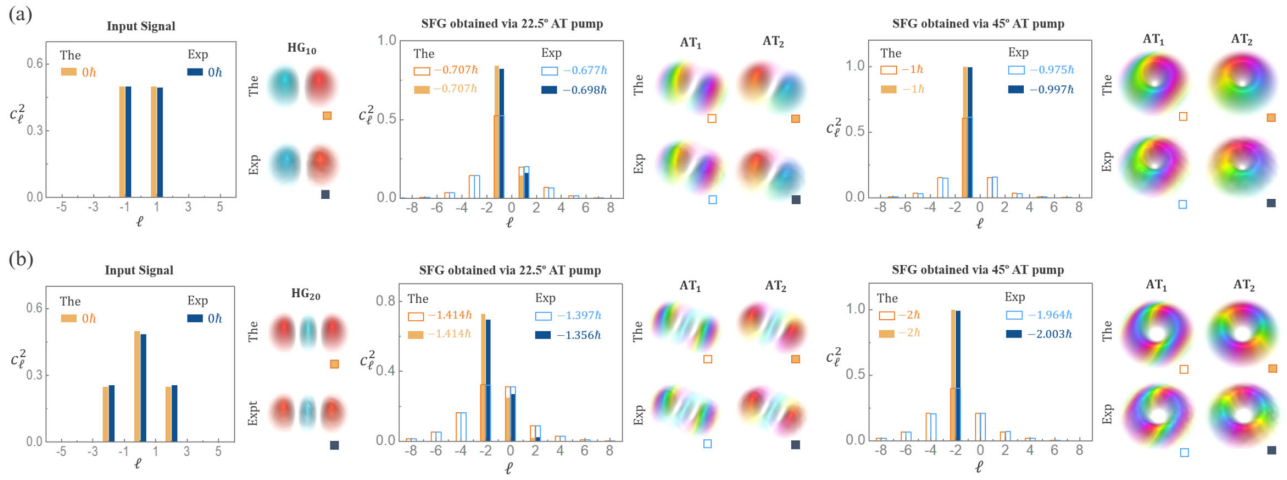

FIG. 3. Simulated and measured OAM spectra of the input HG signal and associated SFG outputs, as well as their complex amplitudes, where (a) and (b) show the results corresponding to using weak $HG_{1,0}$ and $HG_{2,0}$ modes as signals, respectively. The patterns in AT_1 (AT_2) demonstrate the complex amplitudes of the SFG signal before (after) the second astigmatic transformation, and the unfilled (filled) histograms represent the corresponding uncompressed (compressed) OAM spectra.

signal scenario [37]. Therefore, to verify the hypothesis clearly, we consider a pump depletion case, i.e., a weak pump interacting with strong signals, to clarify the change in the amplitude structure of the residual pump. Note that the residual HG signals are still unchanged in the interaction with a weak flattop pump. To pursue the biggest variation in pump OAM, we assumed that the amplitude of the residual pump was completely depleted by the peak amplitude of the signal.

To reproduce this assumption experimentally, by tuning the average power of the pump (1 mW) and signal (~25/30 mw for HG_{10}/HG_{20}) beams, we ensured that the observed residual pump profiles were as close as possible to the theoretical reference.

Figure 4 shows the measured OAM spectra of the AT pump before and after the depletion interaction, as well as the corresponding complex amplitudes $a_p(\boldsymbol{r})$ and $a_{p'}(\boldsymbol{r})$ observed during the same exposure time. For all cases, the original pump has a perfect flattop amplitude and a symmetric OAM spectrum with respect to the $\ell = 0$ axis, confirming that the beam carries no OAM ($\ell_p = 0$). After the interaction, however, the pump depletion resulted in a reduced amplitude in the interaction regions, exhibiting holes with the same shapes as the HG signal profiles. This

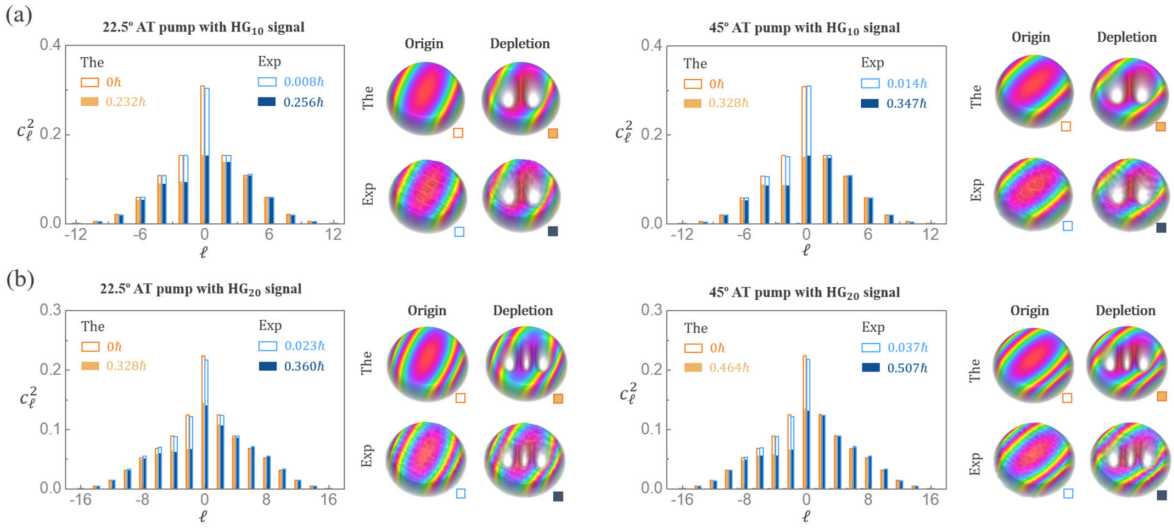

FIG. 4. Simulated and measured OAM spectra of the original (unfilled histograms) and residual (filled histograms) pumps, as well as their complex amplitudes, where (a) and (b) show the results corresponding to using intense $HG_{1,0}$ and $HG_{2,0}$ modes as signals, respectively.

depletion caused the OAM spectra of the residual pump to become asymmetric with respect to $\ell = 0$, which is a feature of a beam carrying net OAM and thus qualitatively confirms the hypothesis.

To quantitatively explore the OAM selection rule, we focus on OAM conservation in the system. This requires the total amount of OAM inflow in the residual pump ($\ell_{p'}$) should be equal to that in the SFG but with the opposite sign, i.e.,

$$\ell_{\mathrm{up}}\bar{n}_{\mathrm{up}} = -\ell_{p'}\bar{n}_{p'}. \tag{4}$$

Here, $\bar{n}_{\mathrm{up}}$ and $\bar{n}_{p'}$ denote the average number of photons contained in the SFG and residual pump, respectively, and their ratio can be calculated with the following equation [37]:

$$\frac{\bar{n}_{\mathrm{up}}}{\bar{n}_{p'}} = \frac{\iint [a_p^2(\boldsymbol{r}) - a_{p'}^2(\boldsymbol{r})]d\boldsymbol{r}}{\iint a_{p'}^2(\boldsymbol{r})d\boldsymbol{r}}, \tag{5}$$

where $a_p^2(\boldsymbol{r})$ and $a_{p'}^2(\boldsymbol{r})$ have the same peak power in plane $\boldsymbol{r}$, corresponding to patterns recorded in experiments by using a camera with the same exposure time. The term $\iint[a_p^2(\boldsymbol{r}) - a_{p'}^2(\boldsymbol{r})]d\boldsymbol{r}$ describes the variation in the pump profile, which is proportional to the amount of photon loss, and the lost photons are converted into SFG signals (i.e., $\bar{n}_{\mathrm{up}}$). By assuming $\iint a_p^2(\boldsymbol{r})d\boldsymbol{r} = 1$, the power of the residual pump $\iint a_{p'}^2(\boldsymbol{r})d\boldsymbol{r}$ in the two cases, i.e., using $\mathrm{HG}_{1,0}$ and $\mathrm{HG}_{2,0}$ modes as signals, are equal to approximately 0.753 and 0.812, respectively, and the corresponding ratios are 0.328 and 0.232 [37]. We can thus use Eq. (4) to obtain the expected average OAM carried by the 45° (22.5°) residual pump, i.e., $\ell_{p'}\hbar$ per photon, which is equal to approximately $0.328\hbar$ ($0.232\hbar$) and $0.464\hbar$ ($0.328\hbar$), respectively. These theoretical predictions, consistent with the measured OAM spectra, confirmed the hypothesis.

The reason for creating OAM beam 'out of the blue' is the nonlinear polarization excited in the crystal has an astigmatic-HG complex amplitude, which emits later a SFG with a LG beam structure. Meanwhile, the amplitude loss in the pump leads to its residue carrying the same amount but opposite OAM, and thus holds the system OAM conservation. Note that despite that the residual pump experienced only an amplitude modulation, its AT wave front cooperates with the amplitude loss and finally results in the OAM inflow.

We report experimentally anomalous OAM conservation in nonlinear AT operations, in which HG signals were upconverted into LG or intermediate HLG modes according to the relative angle of the AT pump. This demonstration provides a useful nonlinear technique for shaping structured light and, more importantly, reveals an unexpected OAM selection rule, namely, that the pump and signal both carry no net OAM, but their SFG does carry OAM, which contradicts the current paradigm. Our results show that the residual pump carries the same amount of OAM as the SFG but with an opposite chirality, thus maintaining OAM conservation in the system. These findings provide deeper insight into OAM conservation in parametric nonlinear systems and indicate that similar phenomena should be explored, such as analogs in parametric amplification and four-wave mixing [11,12,16,25].

The anomalous OAM selection rule revealed here, i.e., creation of two equal but opposite OAM beams via nonlinear interaction without any vortex inputs, can inspire new applications of structured nonlinear optics [7]. Particularly, transfer of spatial phase (or induced coherent) via nonlinear media has enabled many novel imaging techniques [29–32,50]; it can be expected that the new revealed mechanism will certainly bring new nonlinear methods for spatial optical analog computing [51]. Many exciting results in the quantum region could be expected. For instance, the interaction can be regarded as a nonlinear OAM sorter that separates the pump into two frequency bins carrying opposite net OAM. Thus, perhaps it can convert a polarization entanglement into a hybrid one including both frequency and OAM degree of freedoms. Besides, the full even-valued OAM components in the AT pump indicate the astigmatic wave front may be used for shaping the high-dimension state emitting from a spontaneous parametric down-conversion [13,52].

This work was supported by the National Natural Science Foundation of China (Grants No. 62075050, No. 11934013, and No. 61975047) and the High-Level Talents Project of Heilongjiang Province (Grant No. 2020GSP12).

*zhuzhihan@hrbust.edu.cn
†drshi@ustc.edu.cn

[1] P. A. Franken, A. E. Hill, C. W. Peters, and G. Weinreich, Phys. Rev. Lett. **7**, 118 (1961).
[2] R. W. Boyd, *Nonlinear Optics* (Elsevier, Amsterdam, 2003).
[3] L. Allen, M. W. Beijersbergen, R. J. C. Spreeuw, and J. P. Woerdman, Phys. Rev. A **45**, 8185 (1992).
[4] H. Rubinsztein-Dunlop, A. Forbes, M. V. Berry, M. R. Dennis, D. L. Andrews, M. Mansuripur, C. Denz, C. Alpmann, P. Banzer, and T. Bauer, J. Opt. **19**, 013001 (2016).
[5] Y. Shen, X. Wang, Z. Xie, C. Min, X. Fu, Q. Liu, M. Gong, and X. Yuan, Light Sci. Appl. **8**, 1 (2019).
[6] Forbes M. de Oliveira M. R. Dennis, Nat. Photonics **15**, 253 (2021).
[7] W. T. Buono and A. Forbes, Opto-Electron. Adv. **5**, 210174 (2022).
[8] J. Wang, F. Castellucci, and S. Franke-Arnold, AVS Quantum Sci. **2**, 031702 (2020).
[9] K. Dholakia, N. B. Simpson, M. J. Padgett, and L. Allen, Phys. Rev. A **54**, R3742 (1996).
[10] J. Courtial, K. Dholakia, L. Allen, and M. J. Padgett, Phys. Rev. A **56**, 4193 (1997).

[11] D. P. Caetano, M. P. Almeida, P. H. S. Ribeiro, J. A. O. Huguenin, B. C. dos Santos, and A. Z. Khoury, Phys. Rev. A **66**, 041801 (2002).
[12] T. Roger, J. J. F. Heitz, E. M. Wright, and D. Faccio Sci. Rep. **3**, 3491 (2013).
[13] A. Z. Khoury, P. H. S. Ribeiro, and K. Dechoum, Phys. Rev. A **102**, 033708 (2020).
[14] F. Kong, H. Larocque, E. Karimi, P. B. Corkum, and C. Zhang, Optica **6**, 160 (2019).
[15] B. S. Yu, C. Y. Li, Y. Yang, C. Rosales-Guzmán, and Z. H. Zhu, Laser Photonics Rev. **16**, 2200260 (2022).
[16] G. Walker, A. S. Arnold, and S. Franke-Arnold, Phys. Rev. Lett. **108**, 243601 (2012).
[17] J. T. Mendonça, B. Thidé, and H. Then, Phys. Rev. Lett. **102**, 185005 (2009).
[18] Z. Zhu, W. Gao, C. Mu, and H. Li, Optica **3**, 212 (2016).
[19] J. Vieira, R. M. G. M. Trines, E. P. Alves, R. A. Fonseca, J. T. Mendonça, R. Bingham, P. Norreys, and L. O. Silva, Phys. Rev. Lett. **117**, 265001 (2016).
[20] Z.-H. Zhu, P. Chen, H.-W. Li, B. Zhao, Z.-Y. Zhou, W. Hu, W. Gao, Y.-Q. Lu, and B.-S. Shi, Appl. Phys. Lett. **112**, 161103 (2018).
[21] H.-J. Wu, H.-R. Yang, C. Rosales-Guzmán, W. Gao, B.-S. Shi, and Z.-H. Zhu, Phys. Rev. A **100**, 053840 (2019).
[22] Y. Tang, K. Li, X. Zhang, J. Deng, G. Li, and E. Brasselet, Nat. Photonics **14**, 658 (2020).
[23] A. G. de Oliveira, N. R. da Silva, R. M. de Araújo, P. H. S. Ribeiro, and S. P. Walborn, Phys. Rev. Appl. **14**, 024048 (2020).
[24] B. P. da Silva, W. T. Buono, L. J. Pereira, D. S. Tasca, K. Dechoum, and A. Z. Khoury, Nanophotonics **11**, 771 (2022).
[25] N. R. da Silva, A. G. de Oliveira, M. F. Z. Arruda, R. M. de Araújo, W. C. Soares, S. P. Walborn, R. M. Gomes, and P. H. S. Ribeiro, Phys. Rev. Appl. **15**, 024039 (2021).
[26] H.-J. Wu, B. Zhao, C. Rosales-Guzmán, W. Gao, B.-S. Shi, and Z.-H. Zhu, Phys. Rev. Appl. **13**, 064041 (2020).
[27] L. Rego, K. M. Dorney, N. J. Brooks, Q. L. Nguyen, C.-T. Liao, J. San Román, D. E. Couch, A. Liu, E. Pisanty, and M. Lewenstein, Science **364**, eaaw9486 (2019).
[28] G. Gui, N. J. Brooks, H. C. Kapteyn, M. M. Murnane, and C.-T. Liao, Nat. Photonics **15**, 608 (2021).
[29] H. Liu, J. Li, X. Fang, Xi. Zhao, Y. Zheng, and X. Chen, Phys. Rev. A **96**, 023801 (2017).
[30] H. Liu, X. Zhao, H. Li, Y. Zheng, and X. Chen, Opt. Lett. **43**, 3236 (2018).
[31] X.-D. Qiu, F.-S. Li, W.-H. Zhang, Z.-H. Zhu, and L.-X. Chen, Optica **5**, 208 (2018).
[32] B. P. da Silva, G. H. dos Santos, A. G. de Oliveira, N. R. da Silva, W. T. Buono, R. M. Gomes, W. C. Soares, A. J. Jesus-Silva, E. J. S. Fonseca, P. H. Souto Ribeiro, and A. Z. Khoury, Optica **9**, 908 (2022).
[33] E. G. Abramochkin and V. G. Volostnikov, J. Opt. A **6**, S157 (2004).
[34] M. W. Beijersbergen, L. Allen, H. E. L. O. Van der Veen, and J. P. Woerdman, Opt. Commun. **96**, 123 (1993).
[35] R. Gutiérrez-Cuevas, M. R. Dennis, and M. A. Alonso, J. Opt. **21**, 084001 (2019).
[36] R. Gutiérrez-Cuevas, S. A. Wadood, A. N. Vamivakas, and M. A. Alonso, Phys. Rev. Lett. **125**, 123903 (2020).
[37] See Supplemental Material at http://link.aps.org/supplemental/10.1103/PhysRevLett.130.153803 for detailed theoretical and experimental methods, which includes Refs. [38–40].
[38] A. Barh, P. J. Rodrigo, L. Meng, C. Pedersen, and P. Tidemand-Lichtenberg, Adv. Opt. Photonics **11**, 952 (2019).
[39] B. Ndagano, I. Nape, M. A. Cox, C. Rosales-Guzman, and A. Forbes, J. Lightwave Technol. **36**, 292 (2018).
[40] A. Selyem, C. Rosales-Guzmán, S. Croke, A. Forbes, and S. F. Arnold, Phys. Rev. A **100**, 063842 (2019).
[41] Notably, the AT operation realized by a cylindrical lens can provide only pseudo zero-order operations because Gouy phase accumulation inevitably occurs on the unfocused axis.
[42] J. A. Rodrigo, T. Alieva, and M. L. Calvo, Opt. Express **17**, 4976 (2009).
[43] R.-Y. Zhong, Z.-H. Zhu, H.-J. Wu, C. R.-Guzmán, S.-W. Song, and B.-S. Shi, Phys. Rev. A **103**, 053520 (2021).
[44] B. Pinheiro da Silva, V. A. Pinillos, D. S. Tasca, L. E. Oxman, and A. Z. Khoury, Phys. Rev. Lett. **124**, 033902 (2020).
[45] H.-J. Wu, B.-S. Yu, Z.-H. Zhu, W. Gao, D.-S. Ding, Z.-Y. Zhou, X.-P. Hu, C. Rosales-Guzmán, Y. Shen, and B.-S. Shi, Optica **9**, 187 (2022).
[46] J.-Q. Jiang, H.-J. Wu, B.-S. Yu, C.-Y. Li, X.-Y. Zhang, X.-P. Hu, B.-S. Shi, and Z.-H. Zhu, J. Opt. **25**, 024004 (2023).
[47] E. Toninelli, B. Ndagano, A. Vallés, B. Sephton, I. Nape, A. Ambrosio, F. Capasso, M. J. Padgett, and A. Forbes, Adv. Opt. Photonics **11**, 67 (2019).
[48] Rosales-Guzmán and A. Forbes, *How to Shape Light with Spatial Light Modulators* (SPIE, Bellingham, 2017).
[49] The one-dimensional OAM spectrum (c_ℓ^2) is contracted from the two-dimensional LG spectrum ($c_{\ell,p}^2$), see Supplemental Material [37] for a detailed measuring principle.
[50] G. Lemos, V. Borish, G. Cole, S. Ramelow, R. Lapkiewicz, and A. Zeilinger, Nature (London) **512**, 409 (2014).
[51] Sajjad Abdollahramezani, Omid Hemmatyar, and Ali Adibi, Nanophotonics **9**, 4075 (2020).
[52] S. Liu, Z. Zhou, S. Liu, Y. Li, Y. Li, C. Yang, Z. Xu, Z. Liu, G. Guo, and B. Shi, Phys. Rev. A **98**, 062316 (2018).